eLIFE elifesciences.org

RESEARCH ARTICLE

# Figures and figure supplements

Optical dopamine monitoring with dLight1 reveals mesolimbic phenotypes in a mouse model of neurofibromatosis type 1

**J Elliott Robinson *et al***

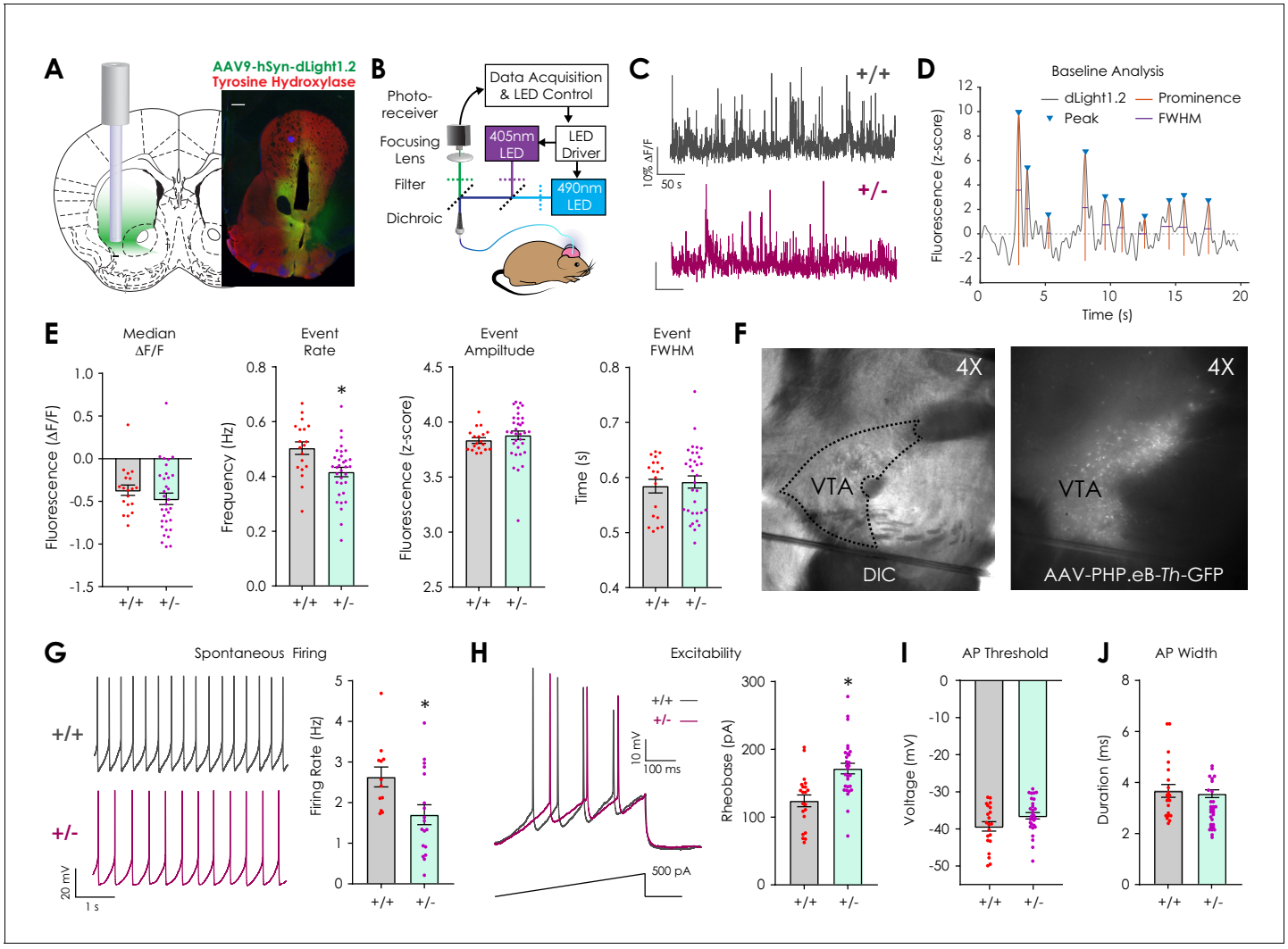


**Figure 1.** Assessment of basal dopaminergic function in vivo with dLight1.2 and ex vivo patch clamp electrophysiology. (**A**) Illustration showing location of stereotaxic injection of the AAV9-hSyn-dLight1.2 viral vector and photometry fiber implantation (*left*). Representative histological image (*right*, scale: 300 µm) showing the fiber tip location and expression of dLight1.2 (stained for GFP, green) and dopaminergic terminal tyrosine hydroxylase (TH, Red). (**B**) Schematic of fiber photometry system used for dLight1.2 (490 nm) and isosbestic (405 nm; reference signal) excitation and emission signal detection in freely moving mice. (**C**) Representative dLight1.2 traces in *Nf1*$^{+/+}$ and *Nf1*$^{+/-}$ mice. (**D**) Representative trace and analysis features for baseline peak detection. (**E**) Peak analysis of baseline dLight1.2 recordings revealed that Nf1$^{+/-}$ mice (n = 33) exhibit reduced transient frequency (unpaired t-test; $t_{50}$ = 3.06, p=0.004) but not median fluorescence (unpaired t-test; $t_{50}$ = 1.01, p=0.32), transient amplitude (unpaired t-test; $t_{50}$ = 0.83, p=0.41), or full width at half maximal amplitude (FWHM; unpaired t-test; $t_{50}$ = 0.43, p=0.67) when compared to Nf1$^{+/+}$ littermates (n = 19). (**F**) 4X differential interference contrast (DIC) image (*left*) of an acute horizontal midbrain slice containing the ventral tegmental area (VTA) and 4X epifluorescence image (*right*) with GFP-labeled catecholaminergic neurons following systemic delivery of AAV-PHP.eB-*Th*-GFP (1 × 10$^{11}$ v.g./mouse). (**G**) Representative traces showing spontaneous whole-cell firing of putative VTA dopaminergic neurons (*left*). Spontaneous firing rates (*right*) were lower (unpaired t-test; $t_{28}$ = 2.58, p=0.0 w) in *Nf1*$^{+/-}$ putative dopaminergic neurons (n = 18) compared to *Nf1*$^{+/+}$ neurons (n = 12). (**H**) Representative electrophysiological traces (*left*) showing evoked firing by a 1 pA/ms ramp current from −60 mV in *Nf1*$^{+/+}$ and *Nf1*$^{+/-}$ putative dopaminergic neurons. Rheobase (*right*; unpaired t-test; $t_{48}$ = 4.05, p<0.001) but not action potential threshold (I; $t_{48}$ = 1.93, p=0.06) or width (J; $t_{48}$ = 0.39, p=0.70) was increased in *Nf1*$^{+/-}$ (n = 29) putative dopaminergic neurons compared to *Nf1*$^{+/+}$ (n = 21). *denotes p<0.05 vs *Nf1*$^{+/+}$. Data presented as mean ± SEM.

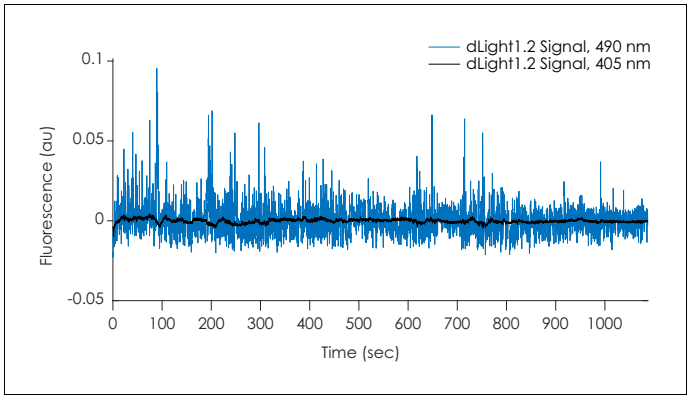


**Figure 1—figure supplement 1.** Raw fluorescent photometry signals. Example traces showing dLight1.2 fluorescence produced by simultaneous isosbestic (405 nm, *black*) or dopamine-dependent (490 nm, *blue*) excitation that were used to calculate the ΔF/F values.

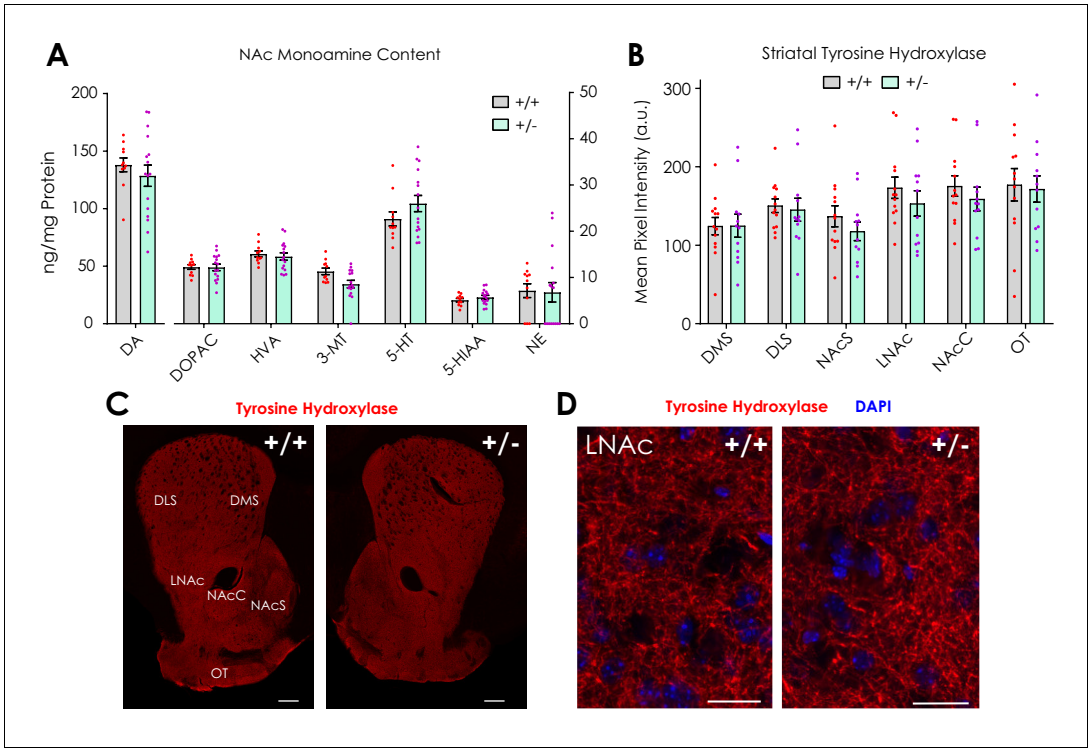


**Figure 1—figure supplement 2.** Striatal catecholamine content and tyrosine hydroxylase immunofluorescence. (**A**) NAc monoamine and monoamine metabolite content determined by HPLC with electrochemical detection (multiple t-tests; $n_{+/+} = 11$; $n_{+/-} = 16$): dopamine (DA; $t_{25} = 0.77$, $q = 0.83$), 3,4-dihydroxyphenylacetic acid (DOPAC; $t_{25} = 0.076$, $q = 0.99$), homovanillic acid (HVA; $t_{25} = 0.52$, $q = 0.90$), 3-methoxytyramine (3-MT; $t_{25} = 2.44$, $q = 0.16$), serotonin (5-HT; $t_{25} = 1.35$, $q = 0.68$), 5-hydroxyindoleacetic acid (5-HIAA; $t_{25} = 1.11$, $q = 0.68$), and norepinephrine (NE; $t_{25} = 0.12$, $q = 0.99$). (**B**) Quantification of TH expression (multiple t-tests; $n_{+/+} = 13$; $n_{+/-} = 12$) in the dorsolateral (DLS; $t_{23} = 0.31$, $q > 0.99$) and dorsomedial striatum (DMS; $t_{23} = 0.029$, $q > 0.99$); lateral nucleus accumbens (LNAc; $t_{23} = 0.96$, $q = 0.88$); nucleus accumbens core (NAcC; $t_{23} = 0.83$, $q = 0.88$) and shell (NAcS; $t_{23} = 1.06$, $q = 0.88$); and the olfactory tubercle (OT; $t_{23} = 0.21$, $q > 0.99$). (**C–D**) Representative fluorescent images showing dopaminergic terminal TH expression in *Nf1*$^{+/-}$ and *Nf1*$^{+/-}$ mice (C scale: 300 μm; D scale: 20 μm). Multiple t-tests were corrected with the two-stage linear step-up procedure of Benjamini, Krieger and Yekutieli with a false discovery rate of 5%. Data presented as mean ± SEM.

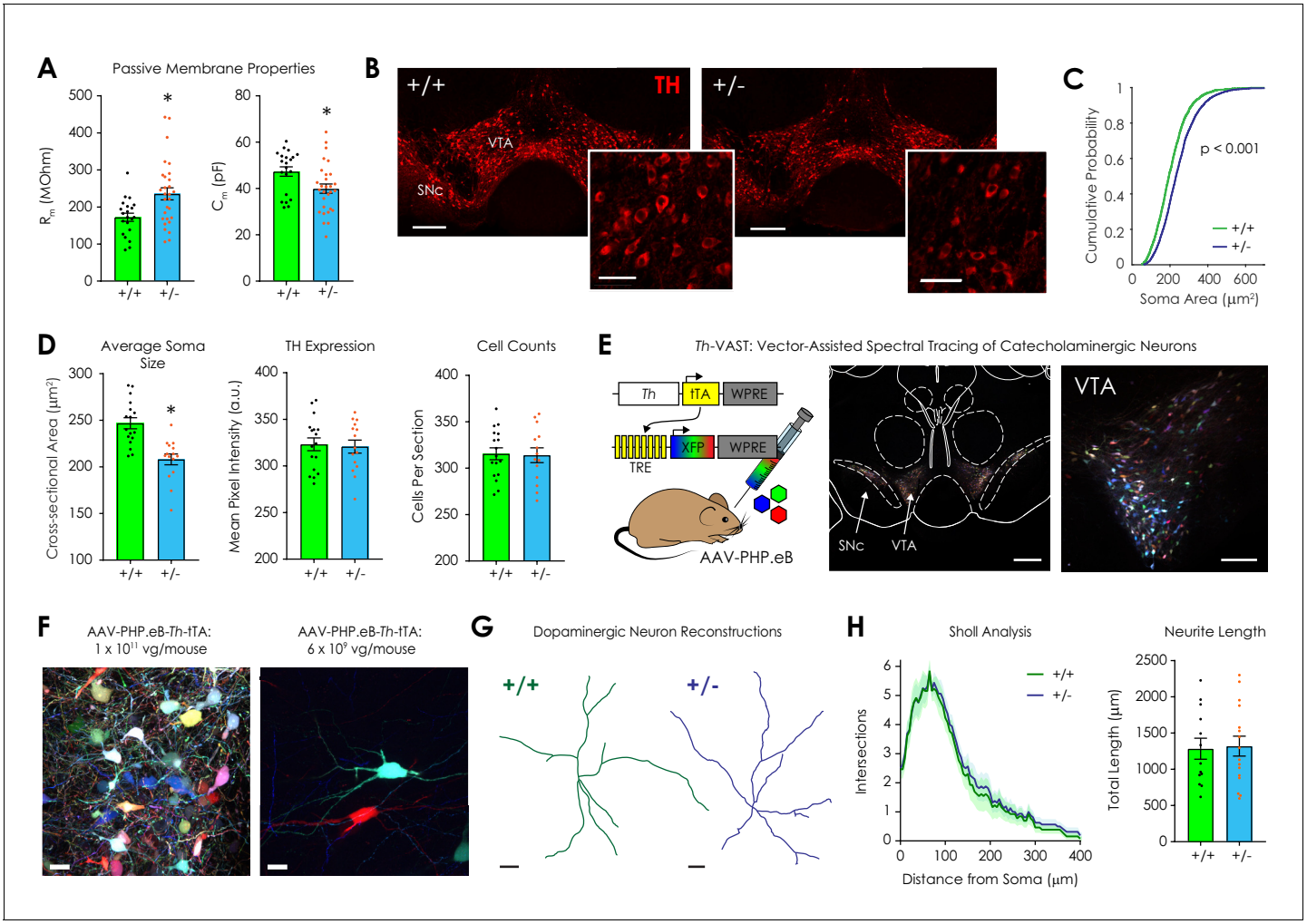


**Figure 2.** Morphological analysis of ventral tegmental dopaminergic neurons in *Nf1*$^{+/+}$ and *Nf1*$^{+/-}$ mice. (**A**) Whole-cell recordings revealed that *Nf1*$^{+/-}$ putative dopaminergic neurons (n = 29) had increased input resistance ($R_m$; *left*; unpaired t-test; $t_{48}$ = 2.97, p=0.005) and decreased capacitance ($C_m$; *right*; $t_{48}$ = 2.54, p=0.01) compared to *Nf1*$^{+/+}$ neurons (n = 21). (**B**) Representative ventral midbrain images containing the ventral tegmental area (VTA) and substantia nigra pars compacta (SNc) stained for tyrosine hydroxylase (TH, scale: 300 µm); TH-positive neurons in the VTA (*inset*, scale: 100 µm). (**C**) The cumulative probability distribution of the cross sectional area of manually traced *Nf1*$^{+/+}$ (n = 2344) and *Nf1*$^{+/-}$ (n = 2586) VTA dopaminergic neuron somata (two-sample Kolmogorov-Smirnov test; D = 0.18, p<0.001). (**D**) Average VTA dopaminergic soma area (*left*; $n_{+/+}$ = 17, $n_{+/-}$ = 15; unpaired t-test; $t_{30}$ = 4.65, p<0.001), TH immunofluorescence (*middle*; $t_{30}$ = 0.25, p=0.90), and number of neurons/histological section (*right*; $t_{30}$ = 0.15, p=0.88) per mouse. (**E**) *Th*-VAST (*left*) produced multicolor labeling of dopaminergic neurons in the VTA (*middle*, scale: 300 µm; *right*, scale: 100 µm). (**F**) Dense (*left*, scale: 20 µm) or sparse multi-color labeling (*right*, scale: 20 µm) was achieved via retro-orbital injection of either 1 × 10$^{11}$ or 6 × 10$^{9}$ vg/mouse AAV-PHP.eB-*Th*-tTA, respectively, and 1 × 10$^{12}$ total vg/mouse of the XFP cocktail (AAV-PHP.eB-TREx7-mRuby2, -mNeonGreen, or -mTurquoise2). (**G**) Representative dopaminergic neuron reconstructions following neurite tracing (scale: 20 µm). (**H**) Sholl analysis failed to detect a difference in dendritic complexity (*left*; two-way repeated measures ANOVA; $F_{80,2160}$ = 0.052, $p_{distance \times genotype}$ >0.99; $F_{80,2160}$ = 63.9, $p_{distance}$ <0.001; $F_{1,27}$ = 0.25, $p_{genotype}$ = 0.63) or total neurite length (*right*; unpaired t-test; $t_{27}$ = 0.18, p=0.86) between genotypes ($n_{+/+}$ = 13, $n_{+/-}$ = 16 for +/- group). * denotes p<0.05 vs *Nf1*$^{+/+}$. Data presented as mean ± SEM.

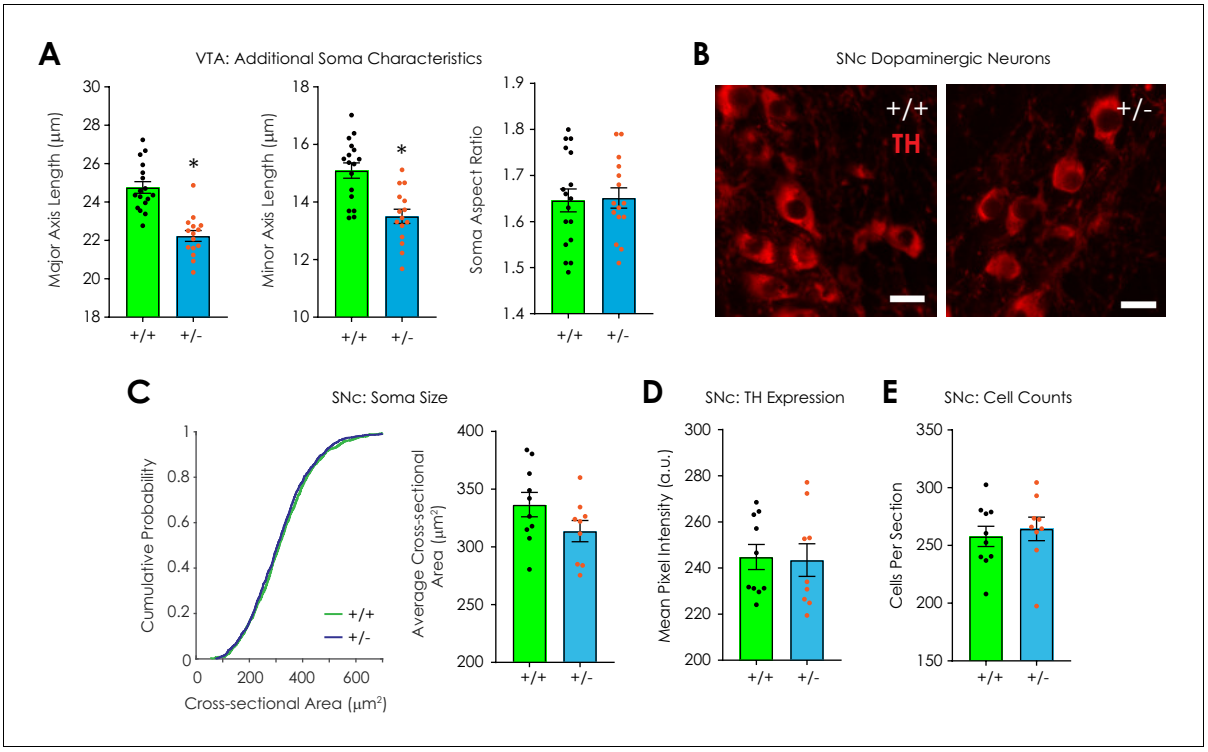


**Figure 2—figure supplement 1.** Additional data: histological analysis. (**A**) *Nf1*$^{+/-}$ dopaminergic neurons (n = 15) have smaller major axis length (*left*; unpaired t-test; $t_{30}$ = 6.06, p<0.001) and minor axis length (*middle*; $t_{30}$ = 4.36, p<0.001) compared to *Nf1*$^{+/+}$ dopaminergic neurons (n = 17) in the VTA; no difference in soma aspect ratio was observed (*right*; $t_{30}$ = 0.16, p=0.87). (**B**) Representative fluorescent images of tyrosine hydroxylase (TH)-labeled dopaminergic neurons in the substantia nigra pars compacta (SNc; scale = 20 µm). (**C**) The cumulative probability distribution of the cross sectional area of manually traced *Nf1*$^{+/+}$ (n = 1131) and *Nf1*$^{+/-}$ (n = 1099) SNc dopaminergic neuron somata (*left*; two-sample Kolmogorov-Smirnov test; D = 0.042, p=0.27). Average SNc dopaminergic soma area (*right*; $n_{+/+}$ = 10; $n_{+/-}$ = 9; unpaired t-test; $t_{17}$ = 1.63, p=0.12). (**D**) Average SNc dopaminergic TH immunofluorescence ($n_{+/+}$ = 10; $n_{+/-}$ = 9; $t_{17}$ = 0.15, p=0.88). (**E**) Average number of dopaminergic neurons/SNc histological section ($n_{+/+}$ = 10; $n_{+/-}$ = 9; $t_{17}$ = 0.49, p=0.63) per mouse. *denotes p<0.05. Data presented as mean ± SEM.

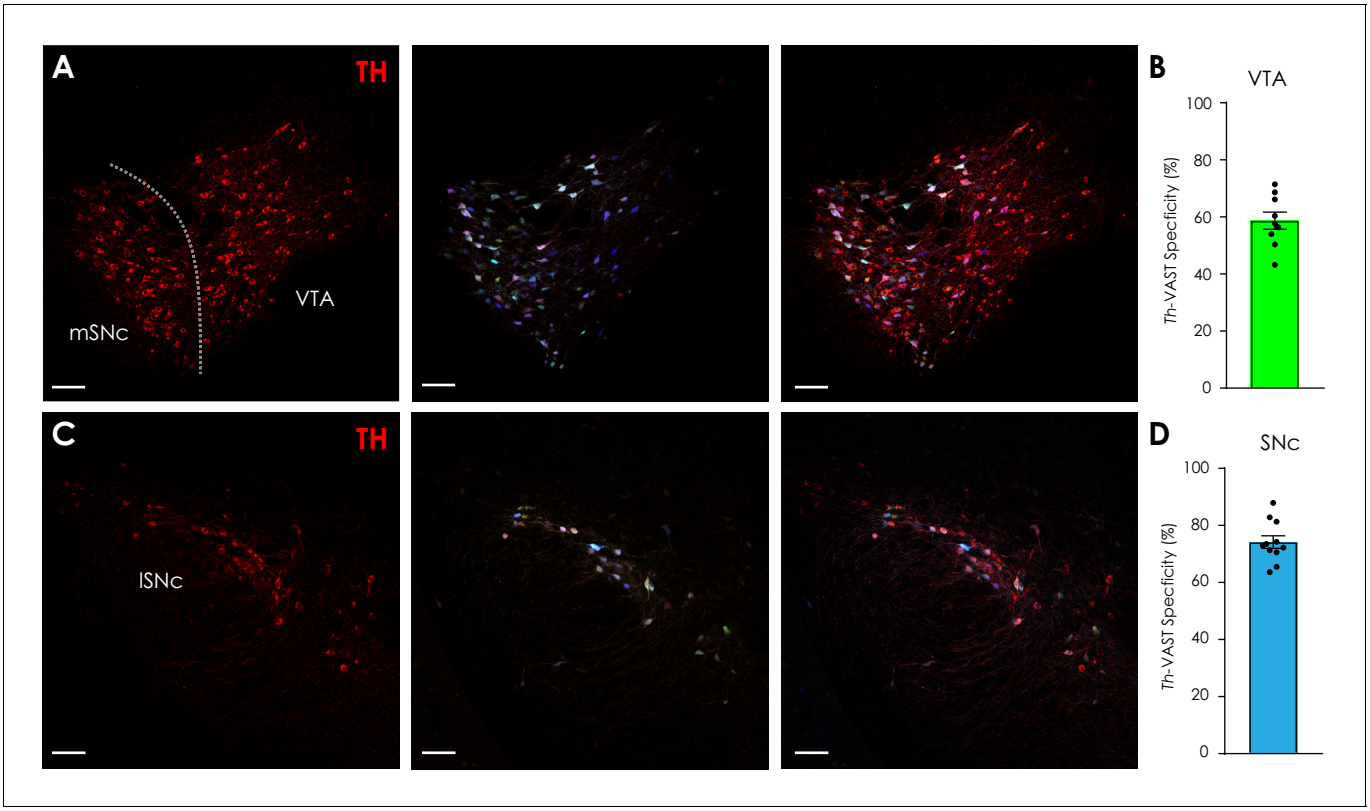


**Figure 2—figure supplement 2.** Additional data: *Th*-VAST. (**A**) Representative confocal images of tyrosine hydroxylase (TH)-stained (*left*) and *Th*-VAST-labeled (*middle*; AAV-PHP.eB-TRE-XFP: $1 \times 10^{12}$ total vg/mouse total, AAV-PHP.eB-*Th*-tTA: $1 \times 10^{11}$ vg/mouse) dopaminergic neurons in coronal sections containing the medial substantia nigra pars compacta (mSNc) and ventral tegmental area (VTA, scale = 100 μm). (*Right*) Overlay. (**B**) Specificity of *Th*-VAST vectors in the VTA was 58.7 ± 3.0%. Each data point represents one histological section. (**C**) Representative confocal images of TH-stained (*left*) and *Th*-VAST-labeled (*middle*; AAV-PHP.eB-TRE-XFP: $1 \times 10^{12}$ total vg/mouse total, AAV-PHP.eB- *Th*-tTA: $1 \times 10^{11}$ vg/mouse) dopaminergic neurons in coronal sections containing the lateral substantia nigra pars compacta (lSNc, scale = 100 μm). (*Right*) Overlay. (**D**) Specificity of *Th*-VAST vectors in the SNc was 74.2 ± 2.2%. Each data point represents one histological section. Data presented as mean ± SEM.

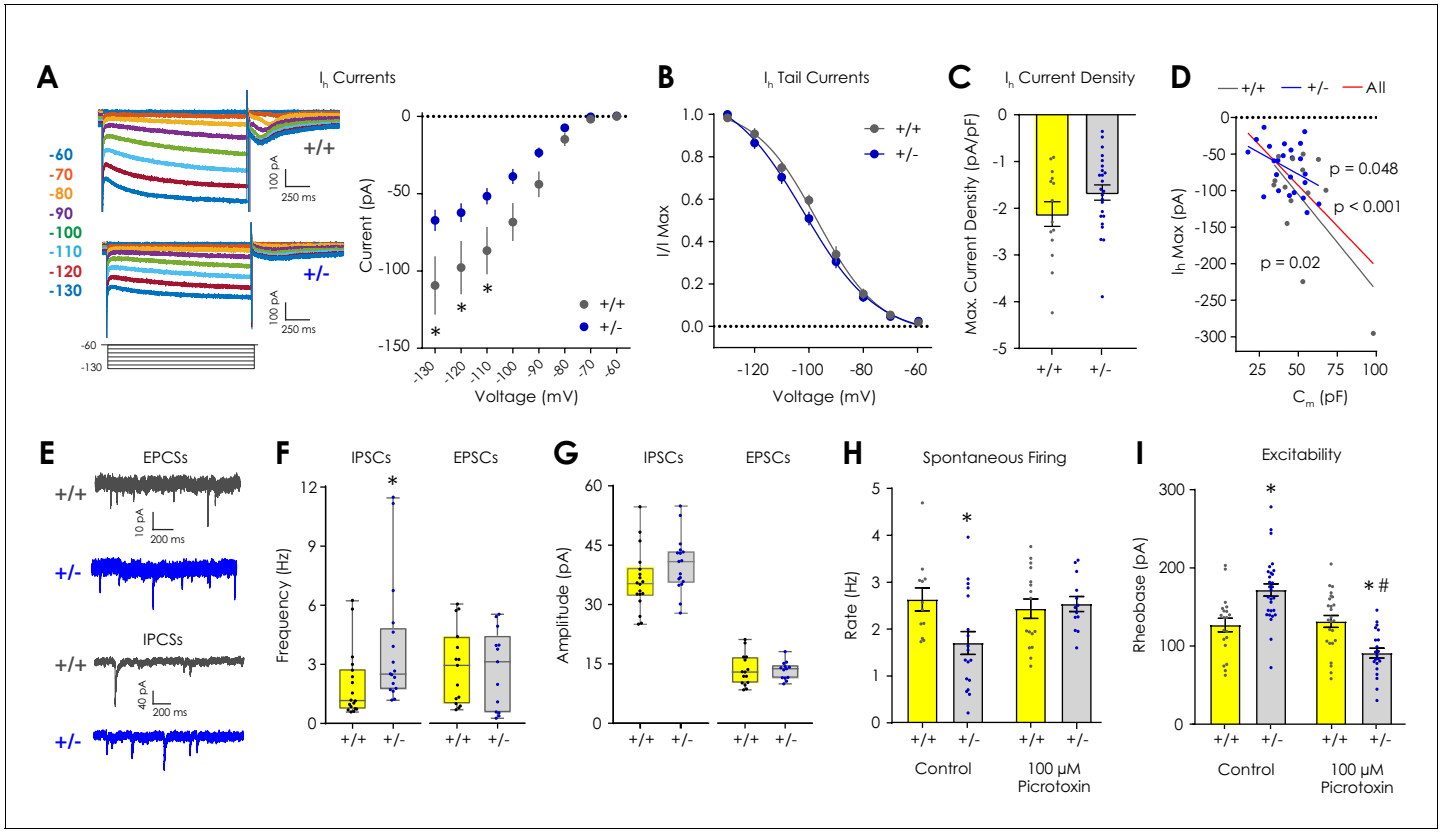


**Figure 3.** Electrophysiological characterization of $I_h$, inhibitory, and excitatory currents in VTA dopaminergic neurons ex vivo. (**A**) Representative traces showing $I_h$ currents during hyperpolarizing voltage steps from −60 to −130 mV. (**B**) $I_h$ current magnitude was smaller (2-way repeated measures ANOVA with Bonferroni post hoc tests; $F_{7,252} = 5.38$, $p_{genotype \times voltage} < 0.001$) in *Nf1*$^{+/-}$ putative dopaminergic neurons (n = 24) compared to *Nf1*$^{+/+}$ neurons (n = 14). (**B**) Tail current analysis showed no difference in the $I_h$ voltage dependence between *Nf1*$^{+/+}$ (n = 14, EV50 = −96.98 mV, 95% CI = −99.69 to −94.52 mV) and *Nf1*$^{+/-}$ putative dopaminergic neurons (n = 24, EV50 = −101.9 mV, 95% CI = −106.5 to −98.86 mV). (**C**) Maximum $I_h$ current density did not differ between *Nf1*$^{+/+}$ (n = 14) and *Nf1*$^{+/-}$ (n = 24) putative dopaminergic neurons (unpaired t-test; $t_{36} = 1.56$, p=0.13). (**D**) $I_h$ magnitude was negatively correlated with $C_m$ in *Nf1*$^{+/+}$ ($R^2 = 0.39$, p=0.02), *Nf1*$^{+/-}$ ($R^2 = 0.17$, p=0.049), and across all putative dopaminergic neurons ($R^2 = 0.35$, p<0.001). (**E**) Representative traces of spontaneous excitatory (sEPSC) and inhibitory (sIPSC) post-synaptic currents. (**F**) The frequency of sIPSCs ($n_{+/+} = 18$, $n_{+/-} = 17$; Mann-Whitney U test; $U = 74.5$, p=0.009; unpaired t-test; $t_{33} = 2.20$, p=0.03) but not sEPSCs ($n_{+/+} = 15$, $n_{+/-} = 13$; $U = 87.0$, p=0.65; $t_{26} = 0.19$, p=0.85) was lower in *Nf1*$^{+/-}$ putative dopaminergic neurons. (**G**) Amplitude of sIPSCs ($n_{+/+} = 18$, $n_{+/-} = 17$; $U = 96.5$, p=0.06; $t_{33} = 1.63$, p=0.11) and sEPSCs ($n_{+/+} = 15$, $n_{+/-} = 13$; $U = 90.0$, p=0.75; $t_{26} = 0.07$, p=0.94). (**H**) 100 µM picrotoxin rescued spontaneous firing of *Nf1*$^{+/-}$ putative dopaminergic neurons ($n_{+/+} = 16$, $n_{+/-} = 13$; two-way ANOVA with Bonferroni *post hoc* tests; $F_{1,55} = 5.18$, $p_{genotype \times drug} = 0.03$; control: $p_{+/+ \text{ vs } +/-} = 0.03$, picrotoxin: $p_{+/+ \text{ vs } +/-} > 0.99$) relative to control neurons ($n_{+/+} = 12$, $n_{+/-} = 18$) and (**I**) lowered rheobase ($n_{+/+} = 25$, $n_{+/-} = 20$) relative to control *Nf1*$^{+/-}$ neurons ($n_{+/+} = 21$, $n_{+/-} = 24$; $F_{1,91} = 30.0$, $p_{genotype \times drug} < 0.001$; control: $p_{+/+ \text{ vs } +/-} < 0.001$, picrotoxin: $p_{+/+ \text{ vs } +/-} = 0.003$, *Nf1*$^{+/-}$: $p_{control \text{ vs } picrotoxin} < 0.001$). * denotes p<0.05 vs *Nf1*$^{+/+}$. # denotes p<0.05 vs control. Data presented as mean ± SEM, except box plots in F-G.

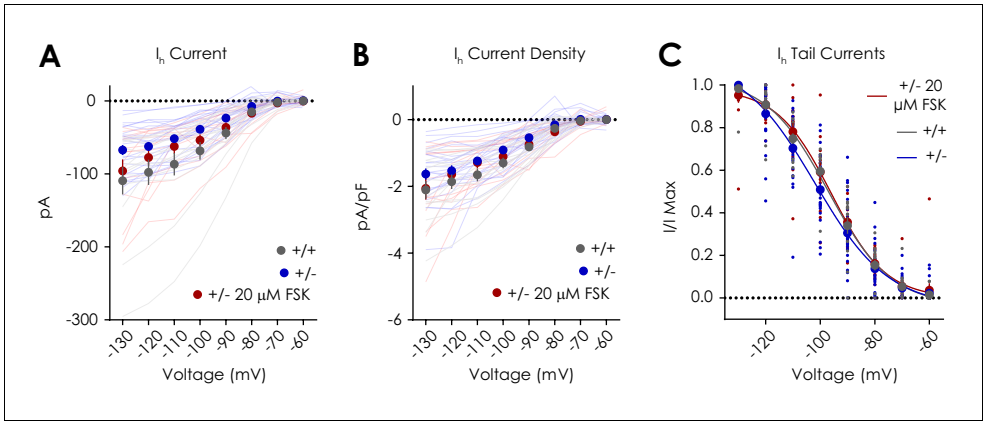


**Figure 3—figure supplement 1.** Effect of 20 µM forskolin (FSK) on putative dopaminergic neuron $I_h$ currents. (**A**) Hyperpolarizing voltage steps from −60 mV to −130 mV evoked voltage-dependent increases in $I_h$ current density that were genotype dependent ($n_{+/+}$ = 14, $n_{+/-}$ = 24, $n_{+/-\ FSK}$ = 14; two-way repeated measures ANOVA with Bonferroni post hoc tests; $F_{14,343}$ = 2.79, $p_{voltage\ x\ treatment\ group}$ <0.001; $F_{7,343}$ = 130.2, $p_{voltage}$ <0.001; $F_{2,49}$ = 3.44, $p_{treatment\ group}$ = 0.04; $p_{+/+\ vs.\ +/-}$ = 0.04; $p_{+/+\ vs.\ +/-\ FSK}$ = 0.92; $p_{+/-\ vs.\ +/-\ FSK}$ = 0.49). (**B**) Voltage-dependent increases in $I_h$ current density ($F_{7,343}$ = 150.2, $p_{voltage}$ <0.001) did not depend on treatment condition ($F_{14,343}$ = 1.12, $p_{voltage\ x\ treatment\ group}$ = 0.33; $F_{2,49}$ = 1.83, $p_{treatment\ group}$ = 0.17; $p_{+/+\ vs.\ +/-}$ = 0.21; $p_{+/+\ vs.\ +/-\ FSK}$ > 0.99; $p_{+/-\ vs.\ +/-\ FSK}$ = 0.79). (**C**) 20 µM forskolin did not affect the voltage dependence of $I_h$ in *Nf1*$^{+/-}$ (n = 14; EV50 = −95.96 mV; 95% CI = −98.93 to −93.11 mV) when compared to control *Nf1*$^{+/+}$ (n = 14; EV50 = −96.98 mV; 95% CI = −99.69 to −94.52 mV) and *Nf1*$^{+/-}$ (n = 24; EV50 = −101.9 mV; 95% CI = −106.5 to −98.86 mV) putative dopaminergic neurons. Data presented as mean ± SEM.

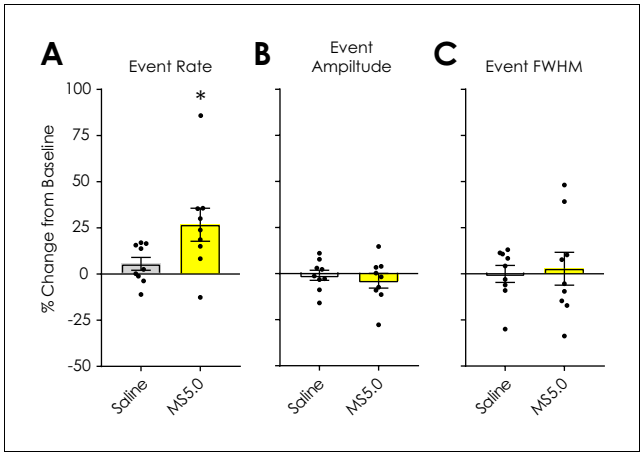


**Figure 3—figure supplement 2.** Effect of 5 mg/kg morphine sulfate on spontaneous dLight1.2 transients in *Nf1*$^{+/-}$ mice. (**A**) Pre-treatment with 5.0 mg/kg (s.c.) morphine sulfate (MS5.0) increased dLight1.2 transient rate versus saline pre-treatment (paired t-test; $t_8 = 2.65$, p=0.03) in *Nf1*$^{+/-}$ mice (n = 9). (**B**) Morphine had no effect on dLight1.2 transient amplitude ($t_8 = 0.82$, p=0.44) or (**C**) full width at half maximal amplitude (FWHM; $t_8 = 0.40$, p=0.70). Data presented as mean ± SEM.

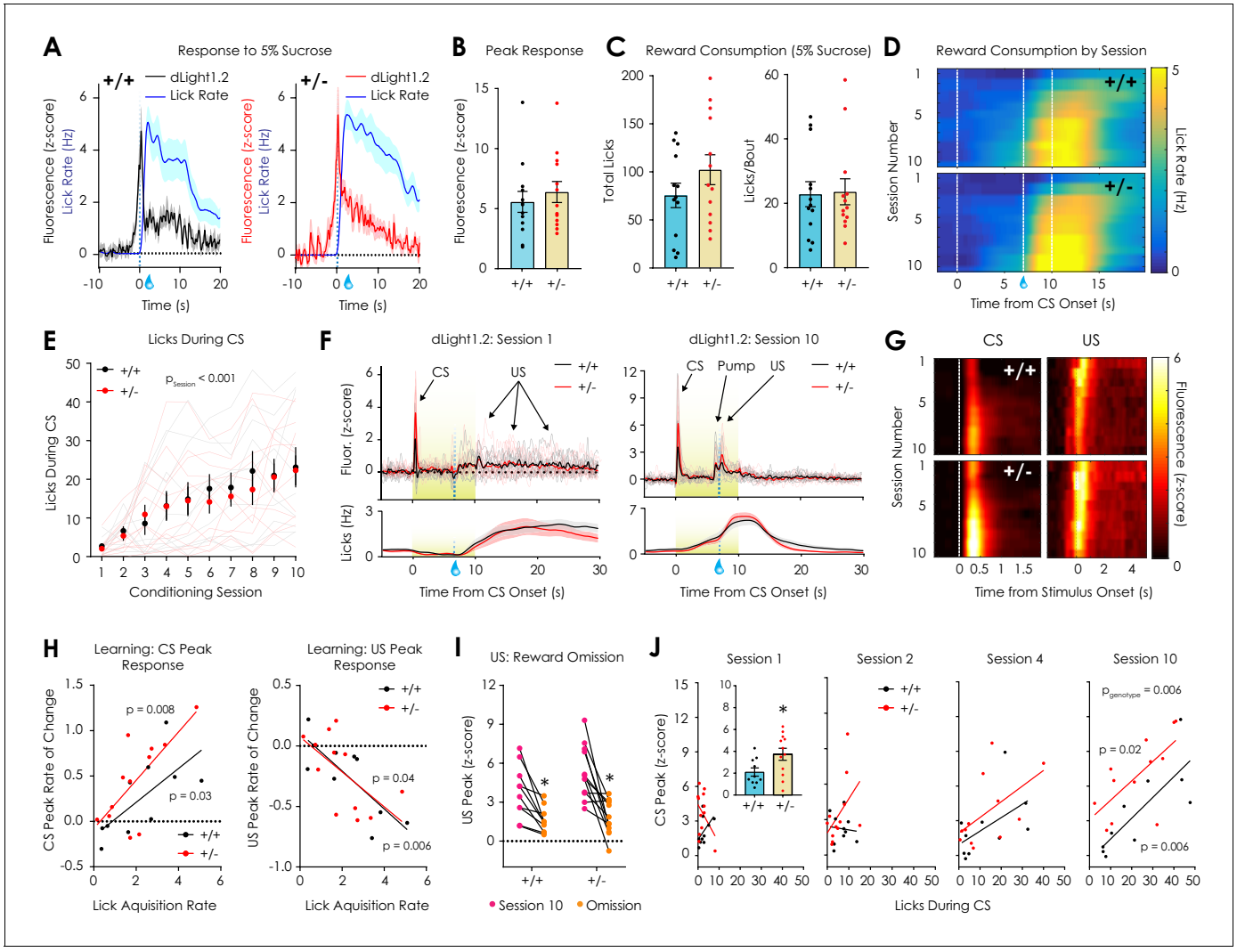


**Figure 4.** In vivo optical monitoring of dopamine dynamics during reward consumption and Pavlovian conditioning. (**A**) Consumption of 5% sucrose evoked robust, time-locked fluorescent dopamine transients in both *Nf1*$^{+/+}$ (*left*) and *Nf1*$^{+/-}$ mice (*right*). (**B**) Peak dLight1.2 responses to the onset sucrose consumption ($n_{+/+}$ = 13, $n_{+/-}$ = 13; unpaired t-test; $t_{24}$ = 0.66, p=0.51). (**C**) No difference in total number of licks (*left*; $t_{24}$ = 1.33, p=0.20) or licks per bout (*right*; $t_{24}$ = 0.14, p=0.89) were observed between genotypes. (**D**) Average session-by-session reward seeking during Pavlovian conditioning; the unconditioned stimulus (US, 5% sucrose) was delivered 7 s after the onset of a reward-predictive 10 s conditioned stimulus (CS, 5 kHz tone with house light illumination). (**E**) *Nf1*$^{+/+}$ (n = 10) and *Nf1*$^{+/-}$ (n = 12) mice displayed learned licking during the CS that was not dependent on genotype (two-way repeated measures ANOVA; $F_{9,180}$ = 0.48, $p_{genotype\ x\ session}$ = 0.89; $F_{9,180}$ = 21.36, $p_{session}$ <0.001; $F_{1,20}$ = 0.09, $p_{genotype}$ = 0.77). (**F**) Individual averaged dLight1.2 traces before (*left*, Session 1) and after (*right*, Session 10) learning showing CS, US, and pump responses. (**G**) Heatmap showing average dLight1.2 responses to the CS (*left;* two-way repeated measures ANOVA; peak response: $F_{9,180}$ = 0.81, $p_{genotype\ x\ session}$ = 0.61) or US (*right*; peak response: $F_{9,180}$ = 0.49, $p_{genotype\ x\ session}$ = 0.88) across training sessions. (**H**) Across sessions, the rate of acquisition of licking during the CS was correlated with the rate of change of the CS (*Nf1*$^{+/+}$: $R^2$ = 0.48, p=0.03; *Nf1*$^{+/-}$: $R^2$ = 0.52, p=0.008) and US peak (*Nf1*$^{+/+}$: $R^2$ = 0.63, p=0.006; *Nf1*$^{+/-}$: $R^2$ = 0.36, p=0.03) in both genotypes. (**I**) Unexpected omission resulted in a significant reduction in US magnitude in both *Nf1*$^{+/+}$ (n = 10; paired t-test; $t_9$ = 4.03, p=0.003) and *Nf1*$^{+/+}$ mice (n = 12; paired t-test; $t_{11}$ = 4.50, p<0.001). (**J**) Correlation between CS peak response and CS licking during session 1 (*Nf1*$^{+/+}$: $R^2$ = 0.25, p=0.14; *Nf1*$^{+/-}$: $R^2$ = 0.16, p=0.21; $p_{genotype}$ = 0.04; *inset*: average peak; unpaired t-test; $t_{20}$ = 2.34, p=0.03), session 2 (*Nf1*$^{+/+}$: $R^2$ = 0.008, p=0.80; *Nf1*$^{+/-}$: $R^2$ = 0.22, p=0.12; $p_{genotype}$ = 0.14), session 4 (*Nf1*$^{+/+}$: $R^2$ = 0.28, p=0.12; *Nf1*$^{+/-}$: $R^2$ = 0.30, p=0.07; $p_{genotype}$ = 0.26), and session 10 (*Nf1*$^{+/+}$: $R^2$ = 0.63, p=0.006; *Nf1*$^{+/-}$: $R^2$ = 0.46, p=0.02; $p_{genotype}$ = 0.006). * denotes p<0.05. Data presented as mean ± SEM.

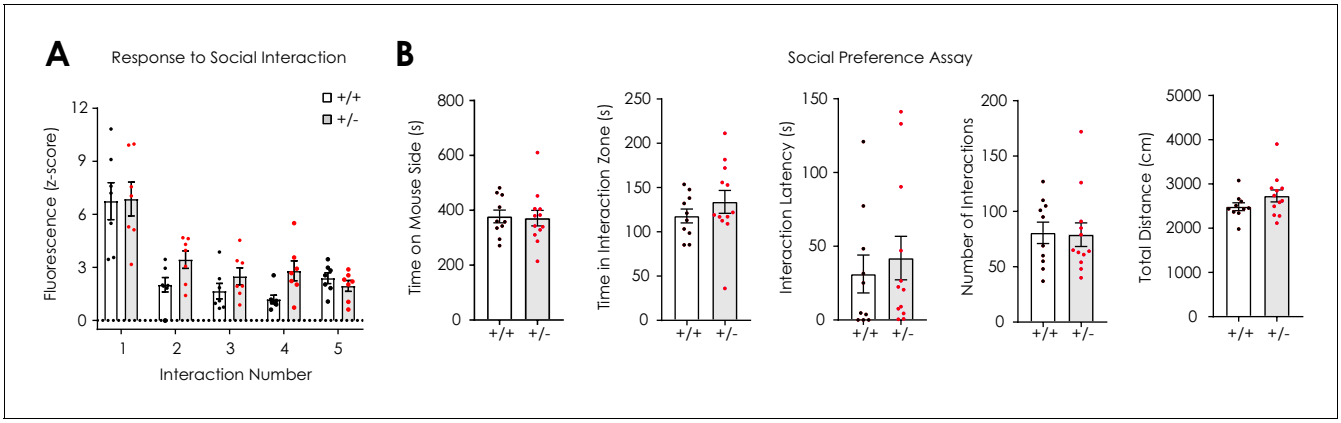


**Figure 4—figure supplement 1.** dLight1.2 responses to social interaction and measurement of social preference. (**A**) dLight1.2 responses to the onset of social interaction decremented from bout to bout ($n_{+/+}$ = 7; $n_{+/-}$ = 7; 2-way repeated measures ANOVA; $F_{4,48}$ = 24.3, $p_{trial}$ <0.001) and did not depend on genotype ($F_{4,48}$ = 1.08, $p_{genotype\ x\ trial}$ = 0.38; $F_{1,12}$ = 4.21, $p_{genotype}$ = 0.06). (**B**) No differences in time on the mouse-paired side (unpaired t-test; $t_{20}$ = 0.16, p=0.87), time in the interaction zone ($t_{20}$ = 1.01, p=0.33), interaction latency ($t_{20}$ = 0.54, p=0.60), number of social interactions ($t_{20}$ = 0.12, p=0.91), or total distance traveled ($t_{20}$ = 1.44, p=0.17) was observed during a social preference assay between *Nf1*$^{+/+}$ (n = 10) and *Nf1*$^{+/-}$ (n = 12) mice. Data presented as mean ± SEM.

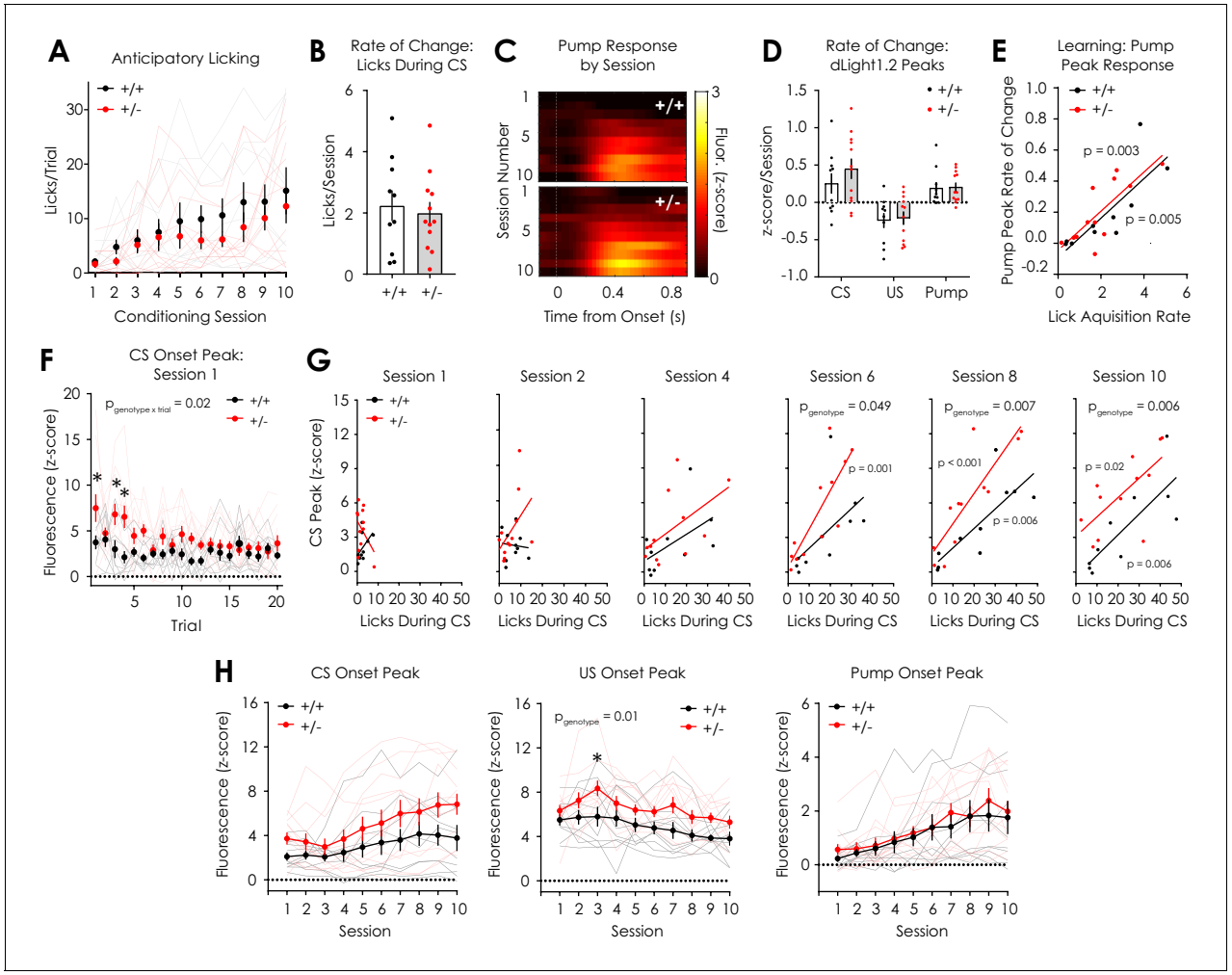


**Figure 4—figure supplement 2.** Additional data: Pavlovian conditioning. (**A**) Anticipatory licking across conditioning sessions ($F_{9,180}$ = 0.39, $p_{genotype\ x\ session}$ = 0.94; $F_{9,180}$ = 9.06, $p_{session}$ <0.001; $F_{1,20}$ = 1.02, $p_{genotype}$ = 0.32) in *Nf1*$^{+/+}$ and *Nf1*$^{+/-}$ mice ($n_{+/+}$ = 10, $n_{+/-}$ = 12). (**B**) No difference in the slope of the linear fit of CS licking across sessions (i.e. the lick acquisition rate) was observed between genotypes during the Pavlovian conditioning task ($n_{+/+}$ = 10, $n_{+/-}$ = 12; unpaired t-test; $t_{20}$ = 0.23, p=0.82). (**C**) Heatmap showing dLight1.2 responses to the sound of the sucrose delivery pump by session. (**D**) No difference between genotypes was observed in the rate of change of the CS (multiple t-tests; $t_{20}$ = 1.00, q = 0.93), US ($t_{20}$ = 0.24, q = 0.93), and pump ($t_{20}$ = 0.14, q = 0.93) peak responses. (**E**) The rate of change of peak pump responses was correlated with lick acquisition rate in both *Nf1*$^{+/+}$ ($R^2$ = 0.64, p=0.005) and *Nf1*$^{+/-}$ ($R^2$ = 0.61, p=0.003) mice independent of genotype ($p_{genotype}$ = 0.47). (**F**) Peak dLight1.2 responses to CS onset during session one decreased on a trial-by-trial basis ($n_{+/+}$ = 10, $n_{+/-}$ = 12; 2-way repeated measures ANOVA with Bonferroni *post hoc* tests; $F_{19,380}$ = 3.07, $p_{trial}$ <0.001) and was greater in *Nf1*$^{+/-}$ mice ($F_{19,\ 380}$ = 2.24, $p_{genotype\ x\ trial}$ = 0.002; $F_{1,20}$ = 6.24, $p_{genotype}$ = 0.02). (**G**) Correlation between CS peak response and CS licking during session 1 (*Nf1*$^{+/+}$: $R^2$ = 0.25, p=0.14; *Nf1*$^{+/-}$: $R^2$ = 0.16, p=0.21; $p_{genotype}$ = 0.04), session 2 (*Nf1*$^{+/+}$: $R^2$ = 0.008, p=0.80; *Nf1*$^{+/-}$: $R^2$ = 0.22, p=0.12; $p_{genotype}$ = 0.14), session 4 (*Nf1*$^{+/+}$: $R^2$ = 0.28, p=0.12; *Nf1*$^{+/-}$: $R^2$ = 0.29, p=0.07; $p_{genotype}$ = 0.27), session 6 (*Nf1*$^{+/+}$: $R^2$ = 0.32, p=0.09; *Nf1*$^{+/-}$: $R^2$ = 0.68, p=0.001; $p_{genotype}$ = 0.049), session 8 (*Nf1*$^{+/+}$: $R^2$ = 0.63, p=0.006; *Nf1*$^{+/-}$: $R^2$ = 0.74, p<0.001; $p_{genotype}$ = 0.007), and session 10 (*Nf1*$^{+/+}$: $R^2$ = 0.63, p=0.006; *Nf1*$^{+/-}$: $R^2$ = 0.46, p=0.02; $p_{genotype}$ = 0.006). (**H**) Peak responses to CS (two-way repeated measures ANOVA with Bonferroni post hoc tests; $F_{9,180}$ = 0.81, $p_{genotype\ x\ session}$ = 0.61; $F_{9,180}$ = 8.47, $p_{session}$ <0.001; $F_{1,20}$ = 2.55, $p_{genotype}$ = 0.13), US ($F_{9,180}$ = 0.50, $p_{genotype\ x\ session}$ = 0.87; $F_{9,180}$ = 5.28, $p_{session}$ <0.001; $F_{1,20}$ = 7.23, $p_{genotype}$ = 0.01), and the sucrose delivery pump ($F_{9,180}$ = 0.30, $p_{genotype\ x\ session}$ = 0.97; $F_{9,180}$ = 11.73, $p_{session}$ <0.001; $F_{1,20}$ = 0.28, $p_{genotype}$ = 0.28) in *Nf1*$^{+/+}$ and *Nf1*$^{+/-}$ mice ($n_{+/+}$ = 10, $n_{+/-}$ = 12). *denotes p<0.05. Multiple t-tests were corrected with the two-stage linear step-up procedure of Benjamini, Krieger, and Yekutieli with a false discovery rate of 5%. Data presented as mean ± SEM.

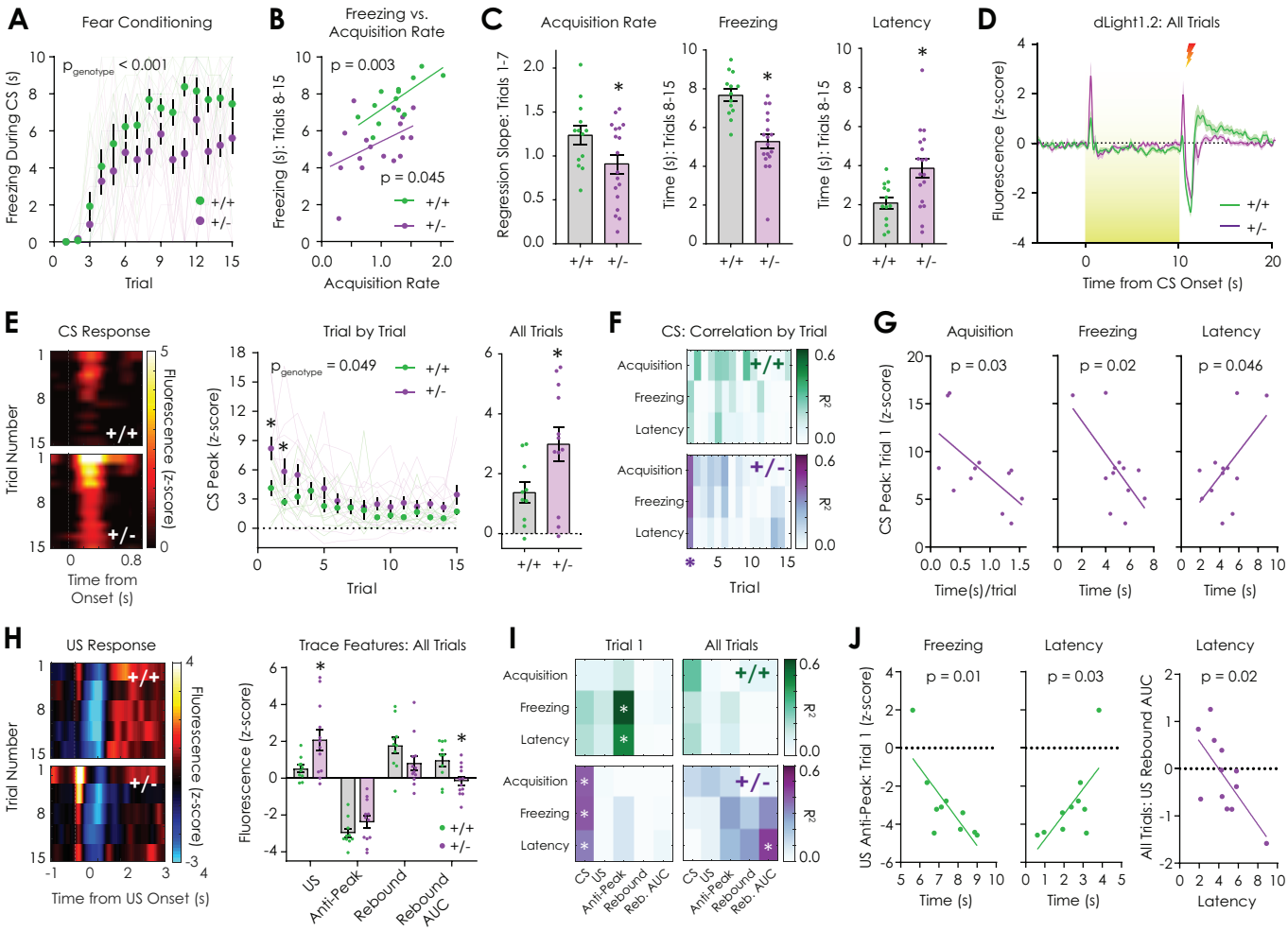


**Figure 5.** In vivo optical monitoring of dopamine dynamics during cued fear conditioning. (**A**) During the cued fear conditioning assay, mice displayed a trial-by-trial increase in freezing that was greater in *Nf1*$^{+/+}$ mice but not dependent on genotype ($n_{+/+}$ = 13, $n_{+/-}$ = 18; 2-way repeated measures ANOVA; $F_{14,406}$ = 1.321, $p_{genotype\ x\ trial}$ = 0.19; $F_{14,406}$ = 28.56, $p_{trial}$ <0.001; $F_{1,29}$ = 18.54, $p_{genotype}$ <0.001). (**B**) The freezing acquisition rate during trials 1–7 was correlated with freezing during trials 8–15 in both *Nf1*$^{+/+}$ (n = 13; $R^2$ = 0.56, p=0.003) and *Nf1*$^{+/-}$ mice (n = 18; $R^2$ = 0.23, p=0.045). (**C**) The freezing acquisition rate (*left*; unpaired t-test; $t_{29}$ = 2.08, p=0.046) and average freezing during trials 8–15 (*middle*; $t_{29}$ = 4.79, p<0.001) were decreased in *Nf1*$^{+/-}$ mice due to increased latency to freeze (*right*; $t_{29}$ = 2.90, p=0.007). (**D**) Averaged dLight1.2 traces showing responses to CS (10 s, 3 kHz tone with house light illumination) presentation and US (1 s, 0.4 mA shock) delivery. (**E**) Heatmaps showing trial-by-trial changes in dLight1.2 signal in response to the CS (*left*). *Nf1*$^{+/-}$ mice (n = 12) displayed increased CS responses across trials (*middle*; two-way repeated measures ANOVA; $F_{14,280}$ = 1.662, $p_{genotype\ x\ trial}$ = 0.06; $F_{14,280}$ = 9.30, $p_{trial}$ <0.001; $F_{1,20}$ = 4.37, $p_{genotype}$ = 0.049) and when traces were averaged (right; unpaired t-test; $t_{20}$ = 2.324, p=0.03) compared to *Nf1*$^{+/+}$ mice (n = 10). (**F**) Correlation matrix showing trial-by-trial correlation strength between behavioral measures and CS peak response. (**G**) In *Nf1*$^{+/-}$ mice, there were significant correlations between the CS peak in trial one and the freezing acquisition rate ($R^2$ = 0.40, p=0.03), time spent freezing ($R^2$ = 0.41, p=0.02), and the latency to freeze ($R^2$ = 0.34, p=0.046). (**H**) Heatmaps showing trial-by-trial changes in dLight1.2 signal in response to US delivery (*left*). *Nf1*$^{+/-}$ mice (n = 12) exhibited increased average peak responses (*right*) to US onset ($t_{20}$ = 2.50, q = 0.04) and decreased integrated post-US rebound (area under the curve or AUC; $t_{20}$ = 2.85, q = 0.03) compared to *Nf1*$^{+/+}$ mice (n = 10). (**I**) Correlation matrices displaying strength of US feature peak-behavior correlations during trial one and across trials. (**J**) There were significant correlations between the US anti-peak magnitude in trial one and freezing ($R^2$ = 0.58, p=0.01) or the latency to freeze ($R^2$ = 0.46, p=0.03) in *Nf1*$^{+/+}$ mice and the integrated post-US rebound across all trials and the latency to freeze ($R^2$ = 0.45, p=0.02) in *Nf1*$^{+/-}$ mice. *denotes p<0.05. Multiple t-tests were corrected with the two-stage linear step-up procedure of Benjamini, Krieger, and Yekutieli with a false discovery rate of 5%. Data presented as mean ± SEM.

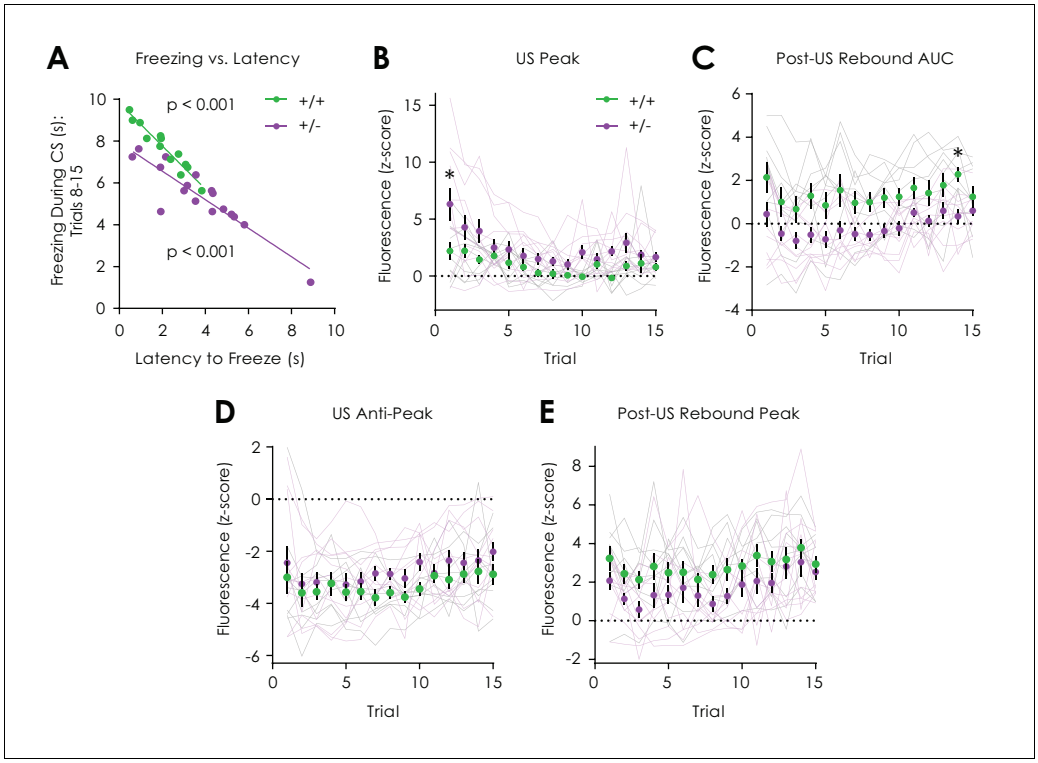


**Figure 5—figure supplement 1.** Additional data: Cued fear conditioning. (**A**) The latency to freeze during trials was correlated with freezing during trials 8–15 in both *Nf1*$^{+/+}$ (n = 13; $R^2$ = 0.93, p<0.001) and *Nf1*$^{+/-}$ mice (n = 18; $R^2$ = 0.82, p<0.001). (**B**) *Nf1*$^{+/-}$ mice (n = 12) displayed increased US responses across trials (two-way repeated measures ANOVA with Bonferroni post hoc tests; $F_{14,280}$ = 1.83, $p_{genotype\ x\ trial}$ = 0.03; $F_{14,280}$ = 8.23, $p_{trial}$ <0.001; $F_{1,20}$ = 6.59, $p_{genotype}$ = 0.02) when compared to *Nf1*$^{+/-}$ littermates. (**C**) The post-US rebound area under the curve (AUC) was greater in *Nf1*$^{+/-}$ mice ($F_{1,20}$ = 8.98, $p_{genotype}$ = 0.007) independent of trial ($F_{14,280}$ = 0.59, $p_{genotype\ x\ trial}$ = 0.87; $F_{14,280}$ = 4.63, $p_{trial}$ <0.001) when compared to *Nf1*$^{+/-}$ littermates. (**D**) No differences in the US anti-peak ($F_{14,280}$ = 0.71, $p_{genotype\ x\ trial}$ = 0.77; $F_{14,280}$ = 3.78, $p_{trial}$ <0.001; $F_{1,20}$ = 1.50, $p_{genotype}$ = 0.24) or (**E**) post-US rebound peak ($F_{14,280}$ = 0.50, $p_{genotype\ x\ trial}$ = 0.93; $F_{14,280}$ = 4.50, $p_{trial}$ <0.001; $F_{1,20}$ = 3.51, $p_{genotype}$ = 0.08) were observed between genotypes. *denotes p<0.05. Data presented as mean ± SEM.

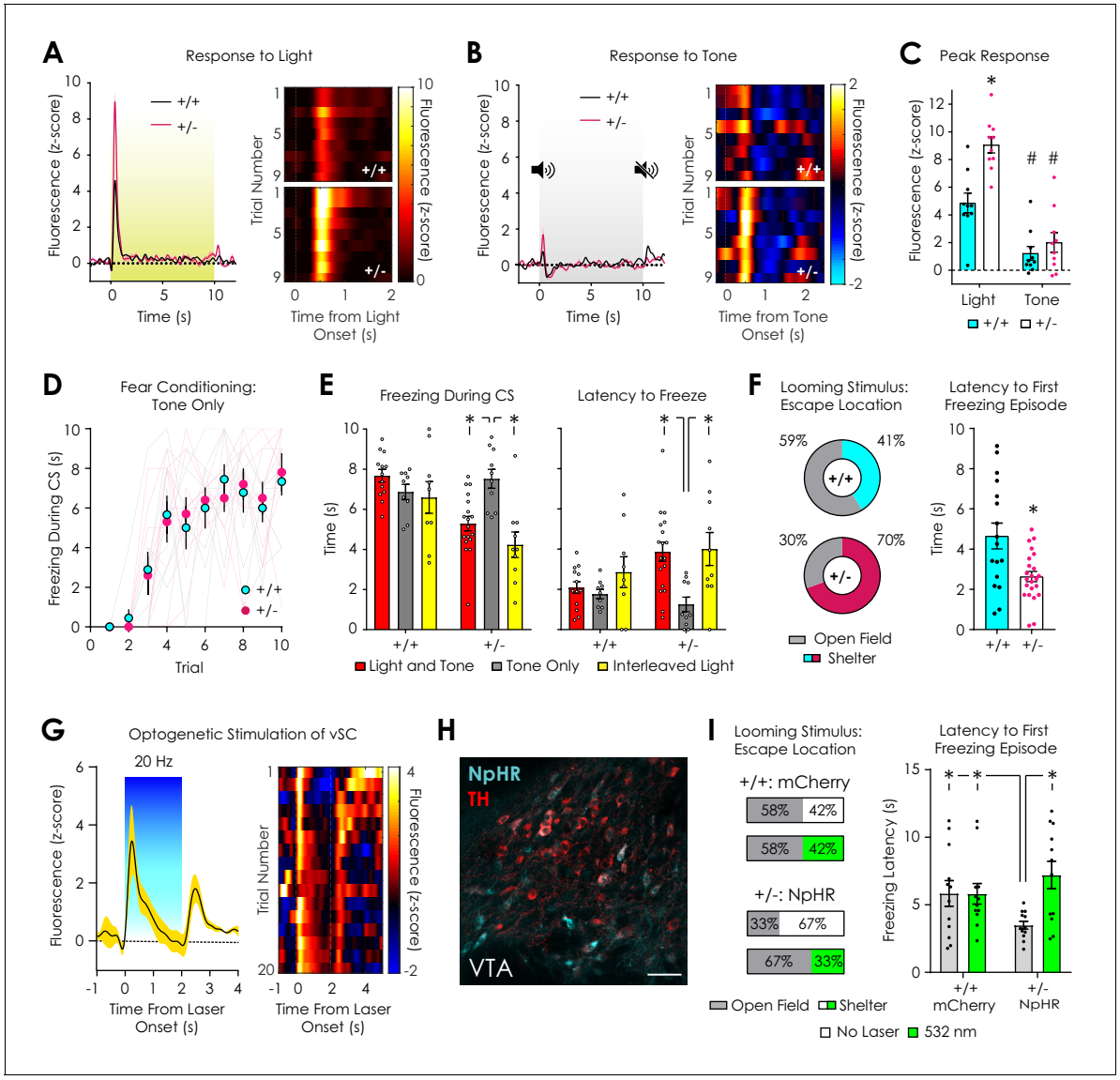


**Figure 6.** Dopaminergic and behavioral responses to salient visual stimuli. (**A**) Average (*left*) and trial-by-trial (*right*) fluorescent dopamine response to a 10 s overhead light stimulus. (**B**) Average (*left*) and trial-by-trial (*right*) fluorescent dopamine response to a 10 s auditory stimulus (5 kHz tone). (**C**) *Nf1*$^{+/-}$ mice had greater peak responses to light ($p<0.001$) but not tone onset ($p>0.99$) compared to *Nf1*$^{+/+}$ mice ($n_{+/+} = 10$, $n_{+/-} = 10$; two-way ANOVA with Bonferroni post hoc tests; $F_{1,36} = 7.27$, $p_{genotype\ x\ condition} = 0.01$; $F_{1,36} = 15.48$, $p_{genotype} <0.001$). In both genotypes, responses to light were greater than responses to tone ($F_{1,36} = 71.02$, $p_{stimulus} <0.001$; $p_{+/+} = 0.002$, $p_{+/-} < 0.001$). (**D**) No difference in cued fear conditioning was observed when a tone-only CS was used ($n_{+/+} = 9$, $n_{+/-} = 10$; two-way repeated measures ANOVA; $F_{9,153} = 0.26$, $p_{genotype\ x\ trial} = 0.98$). (**E**) *Nf1*$^{+/-}$ mice exhibited increased freezing (*left*) and decreased latency to freeze (*right*) in tone-only CS trials (n = 10) compared to light and tone (n = 18; unpaired t-test; freezing: $t_{26} = 3.75$, $p<0.001$; latency: $t_{26} = 3.75$, $p<0.00$) or interleaved light trials (n = 10; paired t-test; freezing: $t_9 = 5.30$, $p<0.001$; latency: $t_9 = 3.48$, $p=0.007$). No differences in freezing or latency to freeze was observed between tone-only CS trials (n = 9) and light and tone (n = 13; unpaired t-test; freezing: $t_{20} = 1.66$, $p=0.11$; latency: $t_{20} = 0.81$, $p=0.43$) or interleaved light trials (n = 10; paired t-test; freezing: $t_8 = 0.42$, $p=0.69$; latency: $t_8 = 1.49$, $p=0.19$) in *Nf1*$^{+/+}$ mice. (**F**) *Nf1*$^{+/+}$ (n = 17) and *Nf1*$^{+/-}$ mice (n = 23) had similar reaction times to a looming stimulus (*left*; $t_{38} = 0.79$, $p=0.43$), yet *Nf1*$^{+/+}$ mice were more likely to escape to the shelter after stimulus presentation (*left*) and exhibited shorter latency to the first freezing episode after looming onset than *Nf1*$^{+/-}$ mice ($t_{38} = 3.24$, $p=0.003$). (**G**) Optogenetic stimulation of the ventral superior colliculus (vSC) produced time-locked dopamine release in the LNAc (n = 3 mice; average trace, *left*; trial-by-trial response, *right*). (**H**) Representative confocal image showing tyrosine hydroxylase (TH)-positive dopaminergic and *Th*-Off-NpHR-eYFP neurons in the VTA (scale: 50 µm). (**I**) In the absence of photoinhibition, VTA$^{Th\text{-}Off\text{-}NpHR\text{-}eYFP}$ *Nf1*$^{+/-}$ mice (n = 12) were more likely to escape to the shelter (*left*) and had shorter latency to the first freezing episode (*right*; unpaired t-test; $t_{22} = 2.36$, $p=0.03$) compared with VTA$^{Th\text{-}Off\text{-}mCherry}$ *Nf1*$^{+/+}$ mice (n = 12). Optogenetic inhibition of VTA$^{non\text{-}Th}$ neurons with 532 nm light (5 mW, 30 Hz, 20 ms pulse width) decreased the probability of escape to the shelter (*left*) and increased the latency to the first freezing episode (*right*; paired t-test; $t_{11} = 3.82$, $p=0.003$) in VTA$^{Th\text{-}Off\text{-}NpHR\text{-}eYFP}$ *Nf1*$^{+/-}$ mice to levels that were similar to VTA$^{Th\text{-}Off\text{-}mCherry}$ *Nf1*$^{+/+}$ mice (unpaired t-test; *Nf1*$^{+/-\ Laser\ On}$ vs *Nf1*$^{+/+\ Laser\ Off}$: $t_{22} = 0.98$, $p=0.34$;

*Figure 6 continued on next page*

*Figure 6 continued*

$Nf1^{+/-\ Laser\ On}$ vs $Nf1^{+/+\ Laser\ On}$: $t_{22} = 1.09$, p=0.29). No difference was observed in $VTA^{Th\text{-}Off\text{-}mCherry}$ $Nf1^{+/+}$ mice between stimulation conditions (paired t-test; $t_{11} = 0.02$, p=0.99). *denotes p<0.05. # denotes p<0.05 vs light stimulus (panel C). Data presented as mean ± SEM.

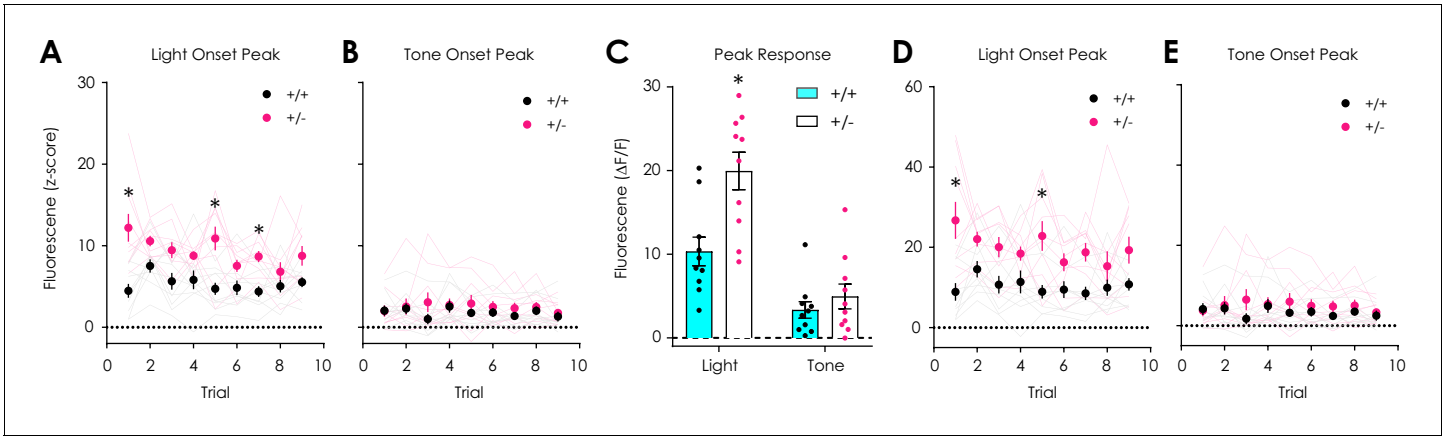


**Figure 6—figure supplement 1.** Additional data: dLight1.2 responses to auditory and visual stimuli. (**A**) dLight1.2 peak responses (z-scored) to overhead light onset were greater in *Nf1*$^{+/-}$ mice (n = 10) versus *Nf1*$^{+/+}$ littermates (n = 10) across trials ($n_{+/+}$ = 10, $n_{+/-}$ = 10; two-way repeated measures ANOVA with Bonferroni post hoc tests; $F_{8,144}$ = 2.78, $p_{genotype\ x\ trial}$ = 0.007). (**B**) No differences in dLight1.2 responses (z-scored) to 60 dB tone were observed across trials ($F_{8,144}$ = 0.92, $p_{genotype\ x\ trial}$ = 0.50). (**C**) *Nf1*$^{+/-}$ mice (n = 10) had greater peak responses (ΔF/F) to overhead light (multiple t-tests; $t_{18}$ = 3.41, q = 0.003) but not tone onset ($t_{18}$ = 0.90, q = 0.19) compared to *Nf1*$^{+/+}$ mice (n = 10). (**D**) dLight1.2 peak responses (ΔF/F) to overhead light onset were greater in *Nf1*$^{+/-}$ mice (n = 10) versus *Nf1*$^{+/+}$ littermates (n = 10) across trials ($n_{+/+}$ = 10, $n_{+/-}$ = 10; two-way repeated measures ANOVA with Bonferroni post hoc tests; $F_{8,144}$ = 2.45, $p_{genotype\ x\ trial}$ = 0.02). (**E**) No differences in dLight1.2 responses (ΔF/F) to 60 dB tone were observed across trials ($F_{8,144}$ = 1.15, $p_{genotype\ x\ trial}$ = 0.33). Multiple t-tests were corrected with the two-stage linear step-up procedure of Benjamini, Krieger and Yekutieli with a false discovery rate of 5%. *denotes p<0.05. Data presented as mean ± SEM.

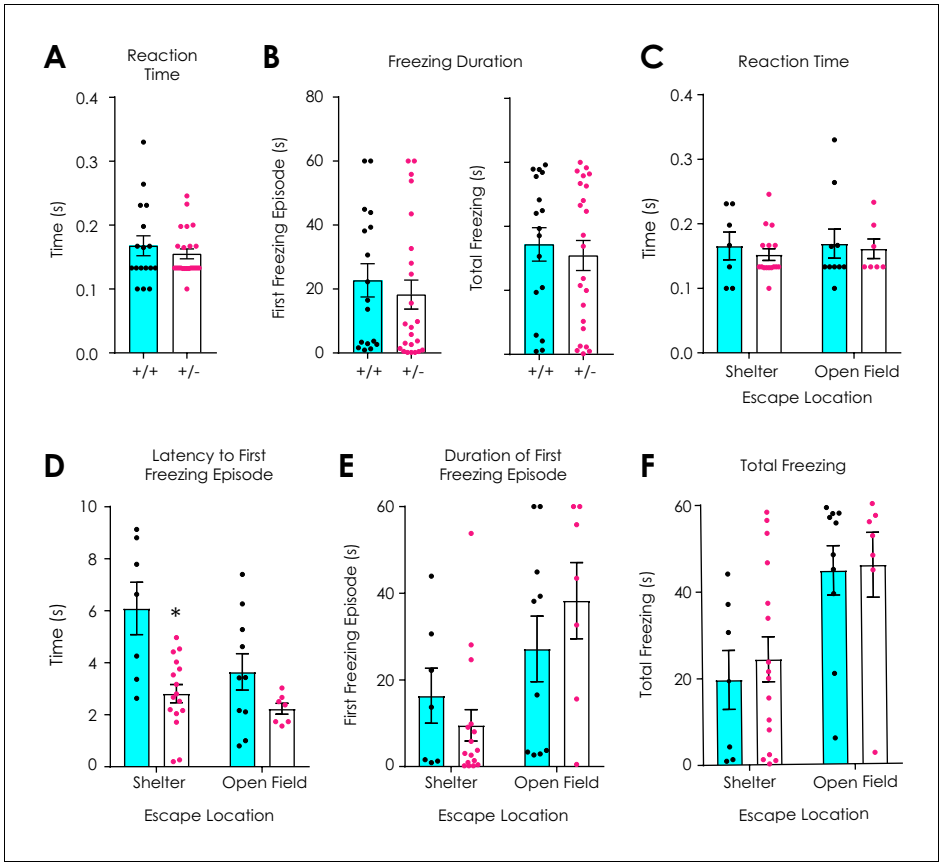


**Figure 6—figure supplement 2.** Additional data: Looming stimulus assay. (**A**) $Nf1^{+/+}$ (n = 17) and $Nf1^{+/-}$ mice (n = 23) have similar reaction times to a looming stimulus ($t_{38}$ = 0.79, p=0.43). (**B**) No difference in the duration of the first freezing episode (*left*; $t_{38}$ = 0.64, p=0.53) or total freezing during the first minute after looming (*right*; $t_{38}$ = 0.49, p=0.62) was observed. (**C**) Reaction time to a looming stimulus did not depend on escape location ($n_{+/+\ shelter}$ = 7, $n_{+/+\ open\ field}$ = 10, $n_{+/-\ shelter}$ = 16, $n_{+/-\ open\ field}$=7; two-way ANOVA with Bonferroni post hoc tests; $F_{1,36}$ = 0.03, $p_{genotype\ x\ location}$ = 0.87; $F_{1,36}$ = 0.13, $p_{location}$ = 0.72; $F_{1,36}$ = 0.38, $p_{genotype}$ = 0.54). (**D**) The latency to the first freezing episode was shorter in $Nf1^{+/-}$ mice ($F_{1,36}$ = 15.0, $p_{genotype}$ <0.001) and independent of freezing location ($F_{1,36}$ = 2.35, $p_{genotype\ x\ location}$ = 0.13), although a significant main effect of location was observed ($F_{1,36}$ = 6.22, $p_{location}$ = 0.02). (**E**) The duration of first freezing episode ($F_{1,36}$ = 1.95, $p_{genotype\ x\ location}$ = 0.17; $F_{1,36}$ = 9.51, $p_{location}$ = 0.004; $F_{1,36}$ = 0.11, $p_{genotype}$ = 0.74) and (**F**) the total time spent freezing during the first minute after looming ($F_{1,36}$ = 0.07, $p_{genotype\ x\ location}$ = 0.79; $F_{1,36}$ = 12.68, $p_{location}$ = 0.001; $F_{1,36}$ = 0.20, $p_{genotype}$ = 0.66) were significantly influenced by freezing location independent of genotype. *denotes p<0.05. Data presented as mean ± SEM.

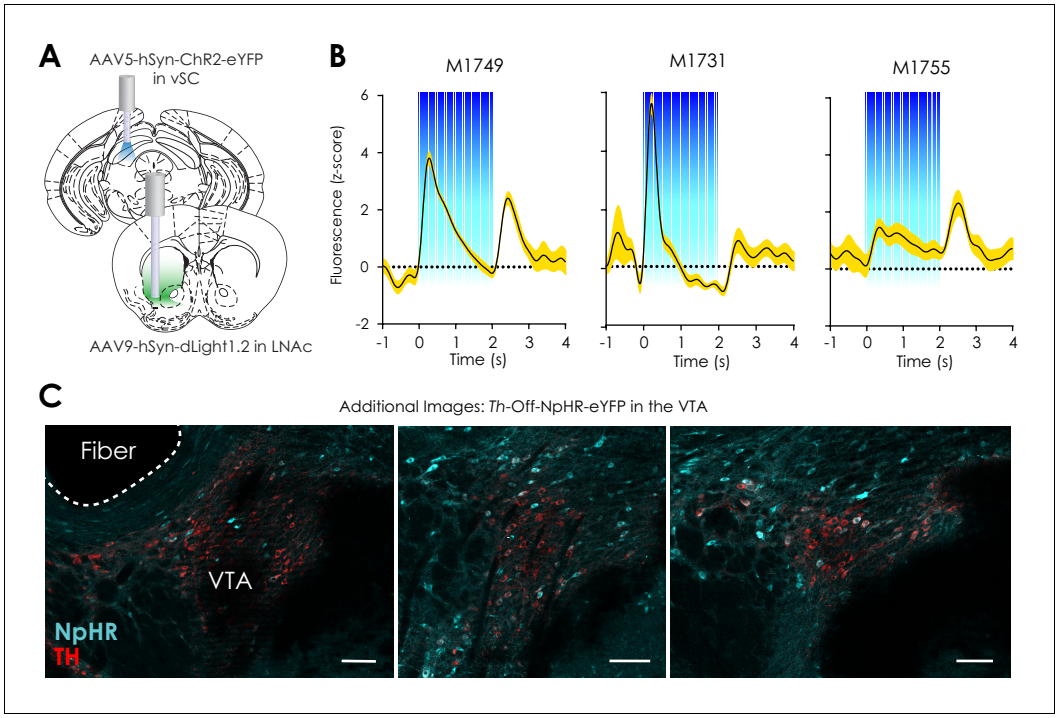


**Figure 6—figure supplement 3.** Additional data: Optogenetic control of the vSC and VTA$^{non\text{-}Th}$ neurons. (**A**) Illustration showing location of stereotaxic injection of the AAV5-hSyn-ChR2-eYFP viral vector and optical fiber in the ventral superior colliculus (vSC), as well as the location of the stereotaxic injection of the AAV9-hSyn-dLight1.2 viral vector and photometry fiber implantation in the LNAc. (**B**) Average fluorescence trace from individual mice showing optical LNAc dopamine signals evoked by activation of ChR2 in the ipsilateral vSC via two seconds of 20 Hz, 5 mW, 5 ms pulse-width, 473 nm laser stimulation. (**C**) Additional images showing *Th*-Off-NpHR-eYFP (cyan) and tyrosine hydroxylase (red)-labeled neurons in the VTA (scale = 50 μm).